# *Modeling of climatically forced sedimentation patterns and sedimentary sequences in the North Atlantic*

# Karl Stattegger and Bernd J. Haupt

Geol.–Paläontontologisches Institut,
Universität Kiel, Germany
E-mail: kstattegger@gpi.uni-kiel.de

Sonderforschungsbereich 313,Univ. Kiel, Germany
E-mail: bjhaupt@sfb313.uni-kiel.de
WWW: http://essc.psu.edu/~bjhaupt

The 3–D forward ocean general circulation model (OGCM) SCINNA (Sensitivity and CIrculation in the Northern North Atlantic) and a sedimentation model SEDLOB (SEDimentation in Large Ocean Basins) are used to simulate the climatically driven Quaternary paleoceanography and sedimentation history of the North Atlantic (Haupt et al. 1994, 1995). The sedimentation model is driven by the thermohaline oceanic circulation and coupled to SCINNA.

In view of numerical experiments in stratigraphy, an efficient model is aimed of simulation of sediment distribution patterns on the sea floor, especially accumulation and erosion of sediments integrated over time intervals long enough to represent the stratigraphic architecture. Based on the stratigraphic record, this architecture is composed of succeeding sequences in a chronostratigraphic time frame.

We use SCINNA and SEDLOB to generate basin–wide glacial and interglacial circulation and sedimentation patterns of the North Atlantic. Sediment accumulation is integrated over time spans covering succeeding cold and warm periods as defined by the high–resolution Plio/Pleistocene sedimentary record. Synthetic stratigraphic sections are obtained from this climatically forced basin fill. Examples with maps and synthetic cross sections are presented for the North Atlantic using stratigraphic data from sediment cores covering the last 2.62 million years.

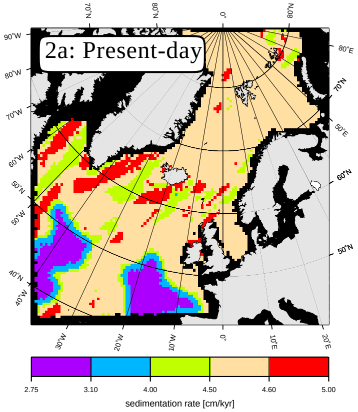


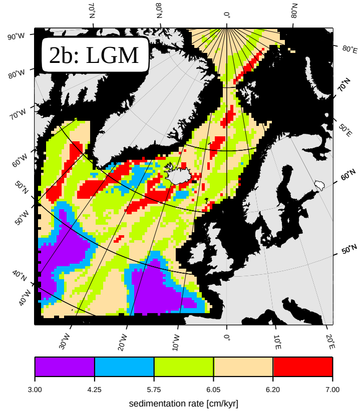


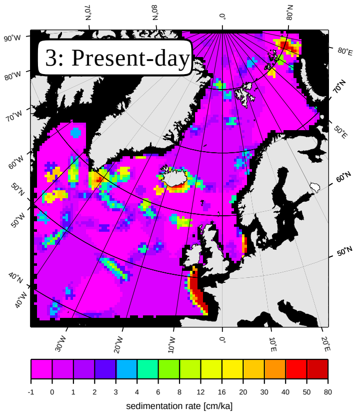


(FIG 2a) Present–day and (FIG 2b) LGM sedimentation rate (centimeters/1000 years). Only the eolian sediment input from the atmosphere (1x10**-13g/cm**2 s) is considered (Miller et al., 1977; Honjo, 1990). The critical velocities for starting of bed load and for beginning of suspension load are set to 0.05 cm $s^{-1}$.

(FIG 3) Present–day sedimentation rate (cm/1000 years). In comparison to experiment HM1 (FIG 4a) additional lateral sediment sources from rivers and coastal melting icebergs are applied (Haupt, 1995; Haupt et al., 1997). Furthermore, the critical velocities for starting of bed load and for beginning of suspension load are set to 0.002 cm $s^{-1}$ respectively 0.02 cm $s^{-1}$ to initiate higher transports.

## scenario 1

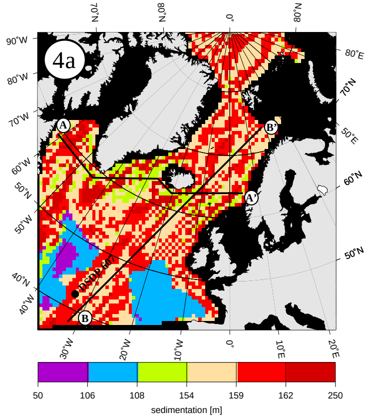


## scenario 2

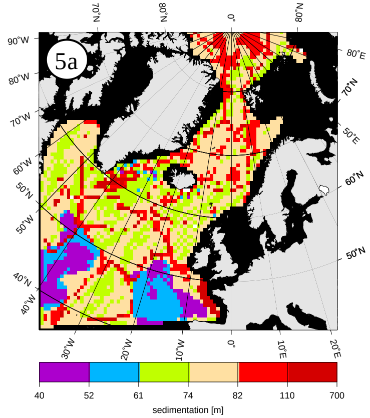


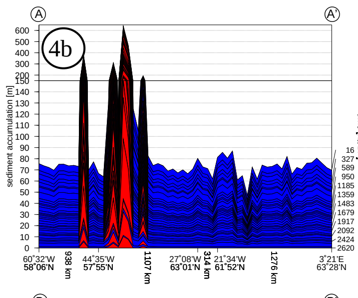


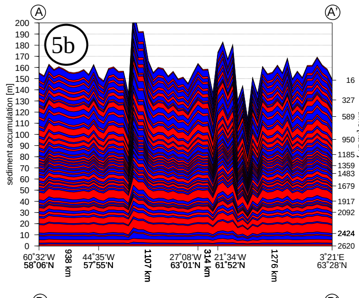


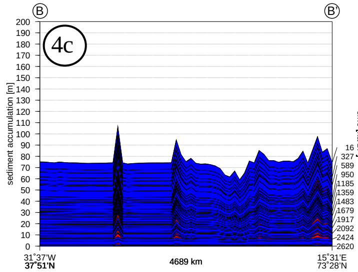


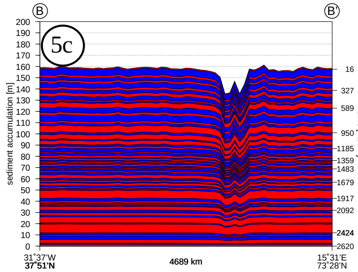


(FIG 4a) Scenario 1: Time–integration and stacking of glacial and interglacial sediment patterns. This scenario uses the sedimentation pattern shown in FIG 2a for the interglacial and that shown in FIG 2b for the glacial state. Additionally, the location of the cross–sections A–A' and B–B' (see FIG 4b, 4c), and the location of the North Atlantic site DSDP 607 (TABLE 1) are shown.

(FIG 4b) Synthetic stratigraphy along the Greenland–Iceland–Faeroer–Scotland Ridge and (FIG 4c) from the Mid–Atlantic Ridge to the border of the Barents shelf in scenario 1 (FIG 4a).

(FIG 5a) Scenario 2: Time–integration and stacking of glacial and interglacial sediment patterns, scenario 1. This scenario uses the sedimentation pattern shown in FIG 3 for the interglacial and that shown in FIG 2b for the glacial state.

| Climatic period | age in ka | duration in ka |
|---|---|---|
| warm | 0–16 | 16 |
| cold | 16–113 | 97 |
| warm | 113–143 | 30 |
| cold | 143–194 | 51 |
| warm | 194–223 | 29 |
| cold | 223–294 | 71 |
| warm | 294 –327 | 33 |
| cold | 327–374 | 47 |
| warm | 374–421 | 47 |
| cold | 421–477 | 56 |
| warm | 477–497 | 20 |
| cold | 497–516 | 19 |
| warm | 516–589 | 73 |
| cold | 589–662 | 73 |
| warm | 662–697 | 35 |
| cold | 697–790 | 93 |
| warm | 790–817 | 27 |
| cold | 817–853 | 36 |
| warm | 853–950 | 97 |
| cold | 950–983 | 33 |
| warm | 983–1052 | 69 |
| cold | 1052–1072 | 20 |
| warm | 1072–1128 | 56 |
| cold | 1128–1159 | 31 |
| warm | 1159–1185 | 26 |
| cold | 1185–1242 | 57 |
| warm | 1242–1259 | 17 |
| cold | 1259–1290 | 31 |
| warm | 1290–1319 | 29 |
| cold | 1319–1336 | 17 |
| warm | 1336–1359 | 23 |
| cold | 1359–1377 | 18 |
| warm | 1377–1396 | 19 |
| cold | 1396–1420 | 24 |
| warm | 1420–1445 | 25 |
| cold | 1445–1468 | 23 |
| warm | 1468–1483 | 15 |
| cold | 1483–1518 | 35 |
| warm | 1518–1538 | 20 |
| cold | 1538–1575 | 37 |
| warm | 1575–1624 | 49 |
| cold | 1624–1655 | 31 |
| warm | 1655–1679 | 24 |
| cold | 1679–1695 | 16 |
| warm | 1695–1729 | 34 |
| cold | 1729–1754 | 25 |
| warm | 1754–1775 | 21 |
| cold | 1775–1801 | 26 |
| warm | 1801–1917 | 116 |
| cold | 1917–1960 | 43 |
| warm | 1960–1985 | 25 |
| cold | 1985–2006 | 21 |
| warm | 2006–2022 | 16 |
| cold | 2022–2037 | 15 |
| warm | 2037–2092 | 55 |
| cold | 2092–2131 | 39 |
| warm | 2131–2166 | 35 |
| cold | 2166–2191 | 25 |
| warm | 2191–2278 | 87 |
| cold | 2278–2296 | 18 |
| warm | 2296–2424 | 128 |
| cold | 2424–2454 | 30 |
| warm | 2454–2471 | 17 |
| cold | 2471–2525 | 54 |
| warm | 2525–2576 | 51 |
| cold | 2576–2595 | 19 |
| warm | 2595–2620 | 25 |

(Table 1) North Atlantic site DSDP 607 (Raymo et al., 1989; Ruddiman et al. 1989), following the oxygen isotope timescale of Shackleton et al. (1990), was used for stratigraphic calibration of glacial and interglacial stages. From the astronomically tuned and globally correlated oxygen isotope record (cf. Tiedemann et al., 1994) stages 1 to 104 close to the Matuyama/Gauss magnetic boundary were used, covering the last 2.62 Ma. Cold and warm periods were distinguished based on the oxygen isotope curve. A continuous time sequence of 33 cold and 34 warm periods was elaborated taking into account shifts in the time dependent mean of oxygen isotope values (Mudelsee & Stattegger, 1997) and a minimum duration of 15000 years per period to contribute noticeably to the build–up of the sediment column. This glacial/interglacial sequence provides the time frame for the basin fill stacking succeeding cold/warm sedimentation patterns.

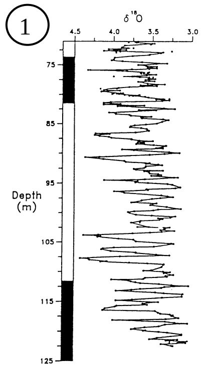


(FIG 1) Site 607 $\delta^{18}O$ record to composite depth, with magnetic polarity of sediments indicated at left (Raymo et al. 1989).